

## Magnetic phase diagram of $\epsilon'$ -FeH HPSTAR 899-2020

Jianjun Ying<sup>1,2,\*</sup>, Jiyong Zhao,<sup>3</sup> Wenli Bi,<sup>3,4,5</sup> E. Ercan Alp,<sup>3</sup> Yuming Xiao,<sup>6</sup>  
Paul Chow,<sup>6</sup> Guoyin Shen,<sup>6</sup> and Viktor V. Struzhkin<sup>7,2,†</sup>

<sup>1</sup>*Department of Physics, and CAS Key Laboratory of Strongly-Coupled Quantum Matter Physics, University of Science and Technology of China, Hefei, Anhui 230026, China*

<sup>2</sup>*Geophysical Laboratory, Carnegie Institution of Washington, Washington, DC 20015, USA*

<sup>3</sup>*Advanced Photon Source, Argonne National Laboratory, Argonne, Illinois 60439, USA*

<sup>4</sup>*Department of Geology, University of Illinois at Urbana-Champaign, Urbana, Illinois 61801, USA*

<sup>5</sup>*Department of Physics, University of Alabama at Birmingham, Birmingham, Alabama 35294, USA*

<sup>6</sup>*HPCAT, X-ray Science Division, Argonne National Laboratory, Argonne, Illinois 60439, USA*

<sup>7</sup>*Center for High Pressure Science and Technology Advanced Research, Shanghai 201203, People's Republic of China*



(Received 19 June 2019; published 14 January 2020)

Iron hydrides attract significant interest as candidates for the main constituents of the Earth's core in geophysics and planetary science. However, their basic physical properties are still not well known. Here, we combined high-pressure transport, synchrotron radiation Mössbauer, and Fe  $K\beta$  x-ray emission spectroscopy measurements on  $\epsilon'$ -FeH to map out a detailed magnetic phase diagram of this hydride phase of iron. In contrast to our original expectations, we found two magnetic phase transitions at high pressure due to two inequivalent iron sites existing in the  $\epsilon'$ -FeH structure. Our results account for the previous large pressure difference on the loss of ferromagnetism between experiment and theoretical calculations. The discovery of an unexpected complex magnetic phase diagram in  $\epsilon'$ -FeH has implications for a better understanding of the magnetic and physical properties of the iron-hydrogen compounds, important for the conditions of planetary interiors.

DOI: [10.1103/PhysRevB.101.020405](https://doi.org/10.1103/PhysRevB.101.020405)

It is believed that the core of our planet is mainly composed of iron-rich alloys with the dissolution of one or more lighter elements [1–3]. Hydrogen has been proposed as a possible major light element in the Earth's core [4–6] because iron hydride ( $\text{FeH}_x$ ) can be formed by a reaction between iron and water under high pressures, however, the exact composition is still uncertain. Thus, detailed investigations of iron hydrides would have significant implications for our understanding of the physics and chemistry of the Earth's core.

Ferromagnetic  $\alpha$ -iron (bcc structure) loses its magnetism under pressures around 13 GPa, concomitant with a structural transition to an hcp structure ( $\epsilon$ -iron) [7]. Meanwhile, superconductivity below 2 K was detected in the nonmagnetic  $\epsilon$ -iron phase [8]. Double hcp (dhcp)  $\epsilon'$ -FeH can be synthesized from a reaction of Fe and fluid  $\text{H}_2$  at high pressures above 3–4 GPa at ambient temperature [9]. The hydrogenation of iron modifies considerably its crystal structure, electric resistivity, and magnetic properties [10,11]. The  $\epsilon'$ -FeH phase exhibits ferromagnetic properties, in contrast to the nonmagnetic high-pressure phase of  $\epsilon$ -Fe. Previous room-temperature synchrotron Mössbauer spectroscopy measurements suggest  $\epsilon'$ -FeH would lose its ferromagnetism above 22–30 GPa [12], which is much lower than the theoretical calculation [13]. However, low-temperature experiments are still missing for tracing the superconductivity and mapping out a detailed magnetic phase diagram. The  $\epsilon'$ -FeH is stable at least up

to 80 GPa, and compression behavior shows an anomaly at 30–50 GPa [14]. However, whether such anomalies are related to the changes in magnetic properties is still unknown. Thus, a detailed investigation of the magnetic properties of  $\epsilon'$ -FeH might be crucial to understanding its high-pressure anomalies. Here, we combined low-temperature transport, synchrotron Mössbauer, and Fe  $K\beta$  x-ray emission spectroscopy (XES) measurements to study in detail the magnetic properties of  $\epsilon'$ -FeH. To our surprise, the magnetism did not completely disappear at low temperatures as reported in previous ambient temperature results. The relative weights of the ordered magnetic moments are decreasing sharply around 26 and 43 GPa. These two anomalies are consistent with the structural anomaly observed in previous work [14]. In addition, the XES result also shows an anomaly above 43 GPa, which indicates a change of iron's local magnetic properties in the course of the second magnetic phase transition. Our results indicate that  $\epsilon'$ -FeH exhibits a much more complex magnetic phase diagram due to the presence of two inequivalent iron sites. These results may have further implications for understanding the physical properties of this iron hydride in planetary interiors.

$\epsilon'$ -FeH samples were prepared by directly loading hydrogen and Fe in a diamond anvil cell. We conducted electrical transport measurements under pressure by using a miniature diamond anvil cell [15]. A diamond anvil with a 300- $\mu\text{m}$  culet and  $c$ -BN gasket with sample chambers of diameter 90  $\mu\text{m}$  were used for the transport measurement. The longitudinal and Hall resistance were measured using the Quantum Design physical property measurement system (PPMS-9) equipment. Synchrotron Mössbauer spectroscopy measurements

\*yingjj@ustc.edu.cn

†vstruzhkin@carnegiescience.edu

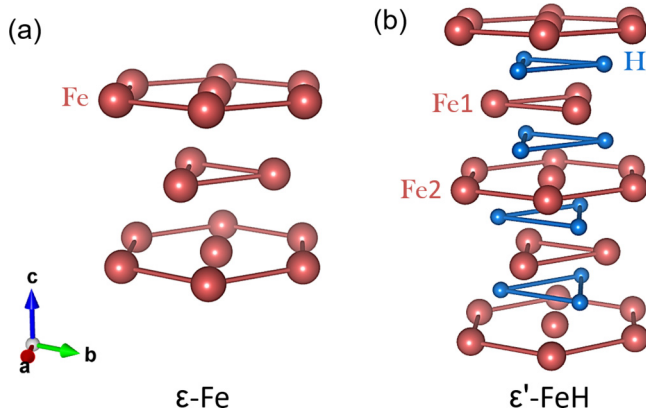


FIG. 1. The crystal structures of (a)  $\epsilon$ -iron and (b)  $\epsilon'$ -FeH. The two crystallographically inequivalent iron sites are labeled as Fe1 and Fe2, respectively.

were performed at 3-IDB at the Advanced Photon Source. A gas membrane-driven miniature panoramic diamond anvil cell and specially designed flow cryostat were used [16,17]. The spectra were fitted by using the CONUSS software [18]. Diamond anvils with a 160- $\mu\text{m}$  culet and Be gasket were used for the x-ray emission spectroscopy (XES) measurements. The room-temperature XES measurements were performed at 16-IDD of the High-Pressure Collaborative Access Team (HPCAT) at the Advanced Photon Source.

The  $\epsilon'$ -FeH structure has an ABAC stacking of Fe triangular layers with hydrogen occupying the octahedral interstitial positions, as shown in Fig. 1. In  $\epsilon'$ -FeH, there are two crystallographically inequivalent iron sites  $2a[\text{Fe}_2, (0, 0, 0)]$  and  $2c[\text{Fe}_1, (1/3, 2/3, 1/4)]$  in the Wyckoff representation. The two inequivalent iron sites would result in two magnetic six-line patterns in the Mössbauer experiment [19,20].

We performed the measurements of the temperature dependence of the resistance under various pressures as shown in Fig. 2. Below 4 GPa, the resistance of iron shows metallic behavior. At high pressure, iron would react with hydrogen and form  $\epsilon'$ -FeH. The resistance increases after the reaction, as previously reported in Ref. [11]. The resistance continuously increases with increasing pressure up to 25 GPa. The resistance starts to gradually decrease above 25 GPa. The reduction of the resistance might be due to the sudden loss of the ferromagnetism in  $\epsilon'$ -FeH above 25 GPa. The resistance exhibits metallic behavior and no superconductivity was discovered down to 2 K at pressures up to 40 GPa.

We also performed Hall measurements at 300 K under various pressures as shown in Fig. 3(a). The giant anomalous Hall effect confirms the ferromagnetism in  $\epsilon'$ -FeH. We can obtain anomalous Hall resistivity  $\rho^{\text{AH}}$  by extrapolating the linear Hall resistivity part at high magnetic field. The maximum value of  $\rho^{\text{AH}}$  is about one order of magnitude larger than in pure iron. Anomalous  $\rho^{\text{AH}}$  rapidly decreases around 25 GPa, and resistance also starts to decrease above that pressure. These results are consistent with the loss of ferromagnetism at high pressures. However,  $\rho^{\text{AH}}$  does not reach zero above 25 GPa, which indicates that the magnetism is not completely suppressed at high pressure. This finding brings up a more complicated magnetic phase diagram than previously thought.

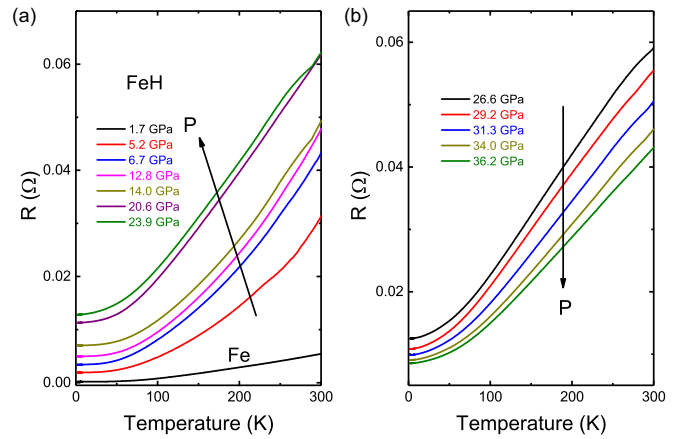


FIG. 2. The temperature dependence of the resistance for  $\epsilon'$ -FeH under various pressures. (a) The resistance increases steeply after the reaction of iron with hydrogen above 4 GPa, and then it increases continuously with increasing pressure. (b) The resistance starts to decrease above 25 GPa, which is due to the magnetic transition. All the resistance curves show metallic behavior and no superconductivity is detected down to 2 K.

In order to investigate the magnetic properties under high pressure, we performed low-temperature synchrotron Mössbauer measurements at high pressure. We show Mössbauer spectra under different pressures and temperatures in Fig. 4. The magnetic low-pressure phase can be fitted by assuming two magnetic Fe sites accompanied by a small portion of the nonmagnetic Fe site ( $<5\%$ ), which may be related to the unreacted nonmagnetic hcp iron. At 300 K, the rapid oscillations related to the ordered magnetic moments suddenly disappear above 26 GPa, which is consistent with previous results [12]. However, with decreasing temperature, the oscillations persist to much higher pressures. The spectra at higher pressures can be fitted by invoking one or two magnetic Fe sites, and one nonmagnetic site. The two different magnetic Fe sites are due to the two inequivalent iron sites in the dhcp phase. We can obtain the magnetic hyperfine fields of both magnetic Fe sites from the fits. From previous Mössbauer results, the hyperfine field of the Fe1 site is slightly larger than on the Fe2 site [19,20], thus we attribute the larger hyperfine field to the Fe1 site in all the fits. The hyperfine fields of both the Fe1 and

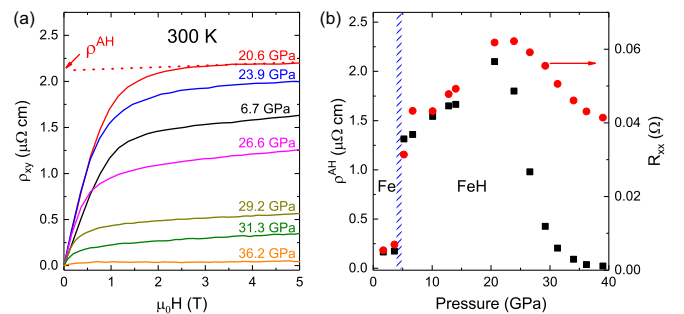


FIG. 3. (a) Anomalous Hall effect as measured at 300 K, which confirms the ferromagnetism in  $\epsilon'$ -FeH. (b) Anomalous Hall resistivity  $\rho^{\text{AH}}$  rapidly decreases around 25 GPa, which is consistent with the loss of ferromagnetism found previously [12].

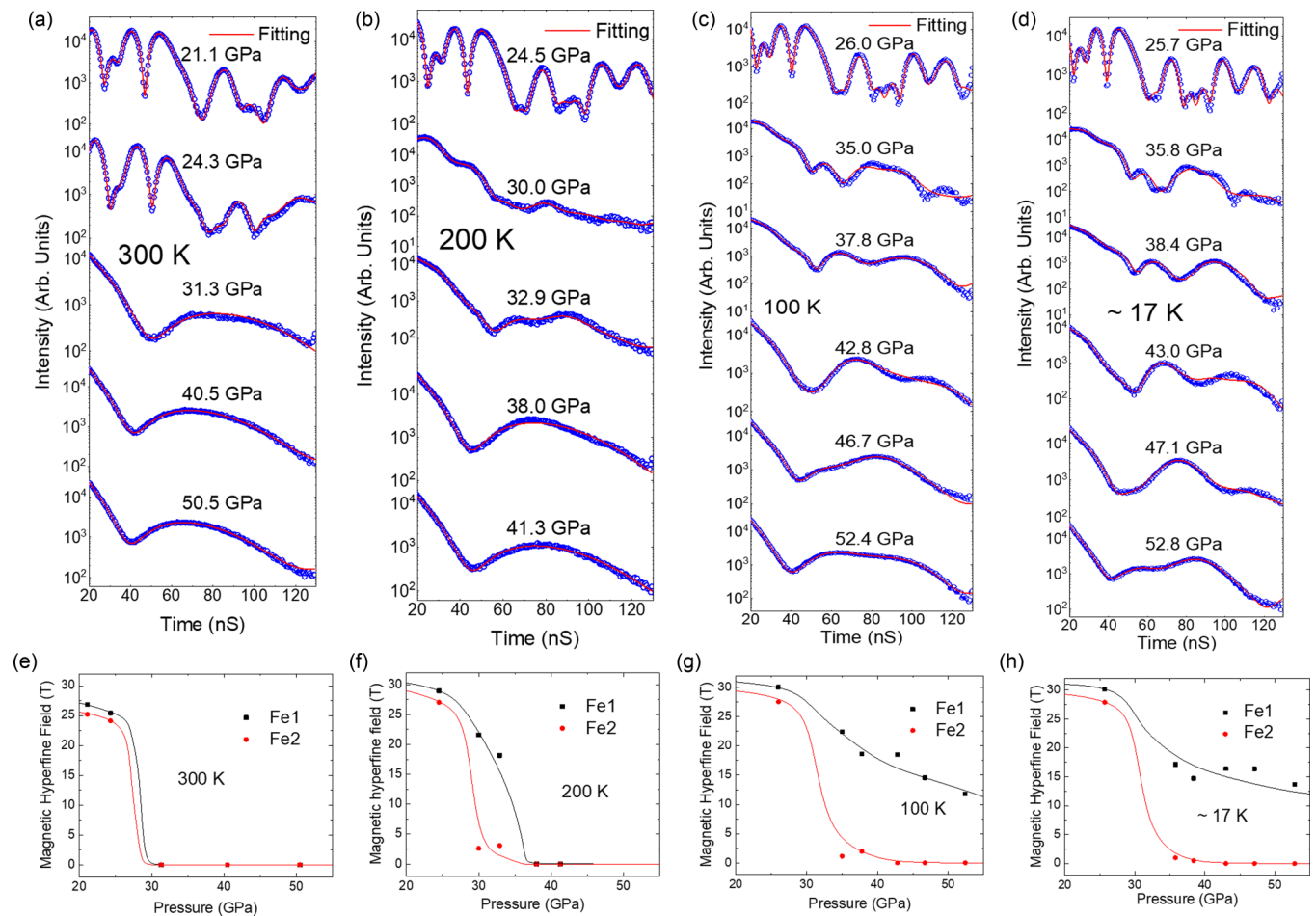


FIG. 4. (a)–(d) High-pressure synchrotron Mössbauer measurements of  $\epsilon'$ -FeH under various temperatures. The red lines are the fits. (e)–(h) The hyperfine magnetic fields at the Fe1 and the Fe2 sites are obtained from the fits. At all temperatures, the hyperfine magnetic fields drop above 26 GPa, however, the value of the hyperfine field at the Fe1 site stays at 15–20 T below 200 K, indicating the remaining magnetism at high pressure. The black and red lines are guides for the eye.

Fe2 sites show a sudden decrease at pressures above 26 GPa. These results are consistent with the loss of ferromagnetism above 26 GPa. However, the hyperfine field of the Fe1 site only drops to  $\sim 20$  T and gradually decreases with increasing pressure at low temperature. These results indicate that the Fe1 and the Fe2 sites show completely different magnetic phase diagrams although their original hyperfine fields are only slightly different.

We can also obtain the weight of ordered moments from the fitting results as shown in Fig. 5. The ordered magnetic part of the Fe1 and the Fe2 sites decreases to 30%–40% above 26 GPa. Above 43 GPa, the weight of the ordered moments shows another sudden decrease at low temperature. Above 43 GPa, a small portion of the ordered moments is still left ( $\sim 4\%$ ) at low temperature and is gradually suppressed with increasing pressure. We can conclude that the first sudden reduction of the ordered moments is mainly related to the loss of magnetism at the Fe2 site. The second sudden decrease above 43 GPa is related to the Fe1 site. In order to extract more information on the magnetic properties of  $\epsilon'$ -FeH under pressure, we performed high-pressure Fe  $K\beta$  XES measurements up to 1 Mbar to probe directly the total local spin properties related to the local magnetic moments. In

order to quantitatively derive the total local moment pressure dependence from the  $K\beta$  line, we used the integrated intensity of the difference spectra around the satellite peak as described in the Supplemental Material [21] (see also Refs. [22,23] therein). The derived portion of the satellite intensity should be proportional to the total local magnetic moment in the material.

Unlike the magnetic transition from  $\alpha$ -iron to  $\epsilon$ -Fe, when the magnetic moment decreases to zero [24], the integrated difference of the normalized spectra of  $\epsilon'$ -FeH does not show any significant anomaly around 26 GPa, which indicates that the local magnetic moment is not quenched at the first magnetic transition. Around the second magnetic transition, the XES shows an anomaly, which indicates that the local magnetic moment changes sharply at the second magnetic transition. Below 43 GPa, the local magnetic moment decreases rapidly with increasing pressure, however, it still has some remaining value at a higher pressure and may be even sustained above 100 GPa.

Our results indicate that the magnetic phase diagram in  $\epsilon'$ -FeH is much more complex than previously thought. There are at least two magnetic phase transitions at high pressure due to the two inequivalent iron sites. The first magnetic transition

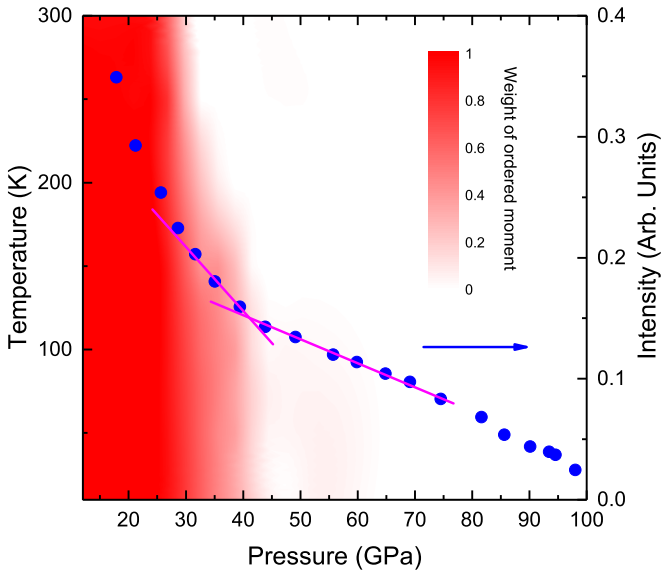


FIG. 5. Magnetic phase diagram of  $\epsilon'$ -FeH. The weight of the ordered moments shows two sharp changes around 26 and 43 GPa, which are related to the two magnetic phase transitions. The deduced difference intensity from the x-ray emission spectroscopy measurements also shows an anomaly around 43 GPa, which indicates that the local magnetic moments are changed in the course of the magnetic phase transition.

is related to the loss of the ferromagnetism at the Fe2 site and a slight decrease of the hyperfine field at the Fe1 site. The second magnetic transition above 43 GPa is related to the loss of magnetic order at the Fe1 site. The remaining small portion of ordered magnetic moments at higher pressure may be related to the disorder in the sample, e.g., due to the presence of stacking faults in the dhcp iron lattice [20]. The discovery of the two magnetic transitions is consistent with the anomalous compression behavior in the range from 30 to 50 GPa [14]. The second magnetic transition explains also the change of the sound velocity slope above 40 GPa in the previous inelastic nuclear resonance x-ray scattering study [12]. From the XES experiment, the local magnetic moment is gradually suppressed with increasing pressure. However, unlike the sudden loss of local moments in compressed Fe,  $\epsilon'$ -FeH still has a remaining local magnetic moment above 43 GPa, although the magnetic ordering is almost suppressed

at these pressures. Our results clearly indicate that  $\epsilon'$ -FeH sustains magnetic ordering and the local magnetic moments in a much broader pressure range than previously expected. Such behavior may be strongly correlated with its particular crystal structure. As we know, the cores of many planets and satellite bodies contain large quantities of iron, including the Earth and Moon. The satellites of Jupiter and Saturn also contain large amounts of water, which could be a source of hydrogen for the formation of iron hydrides. Since hydrogen is the most abundant element in the Universe,  $\epsilon'$ -FeH may form in the interiors of many planetary bodies in our Solar System and across the Universe. Our results of the unexpected magnetic properties of  $\epsilon'$ -FeH may have important implications for understanding the origins and variations of the magnetic fields and magnetic anomalies in the planetary bodies having no liquid core to sustain magnetic dynamo effects. Since we expect that the major form of Fe in gas and icy giant planets is in various hydride phases, FeH may be present in massive eruptions during volcanic activity in the atmospheres of such planets, and may thus be responsible for some of the observed magnetic anomalies in such seismically active zones.

In conclusion, we have mapped out a detailed magnetic phase diagram of  $\epsilon'$ -FeH. Unexpectedly, we find two magnetic phase transitions. This behavior is due to the existence of two inequivalent iron sites, which lose their magnetic ordering at different pressures. Our results account for the large difference in the predicted and observed magnetic collapse pressures between experiment and theoretical calculations. These results may have important implications for understanding the magnetic and physical properties of planetary interiors and magnetic anomalies in gas and icy planets.

HPCAT operations are supported by DOE-NNSA under Award No. DE-NA0001974 and DOE-BES under Award No. DE-FG02-99ER45775, with partial instrumentation funding by NSF. APS is supported by DOE-BES, under Contract No. DE-AC02-06CH11357. Sector 3 operations are partially supported by COMPRES, the Consortium for Materials Properties Research in Earth Sciences under NSF Cooperative Agreement No. EAR-1606856. J.Y. acknowledges support by the CAS Pioneer Hundred Talents Program. V.V.S. acknowledges support from the Thousand Talent Program by the State Council of the People's Republic of China.

- [1] F. Birch, *J. Geophys. Res.* **57**, 227 (1952).
- [2] H.-K. Mao, Y. Wu, L. C. Chen, and J. F. Shu, *J. Geophys. Res.* **95**, 21737 (1990).
- [3] R. Jeanloz, *Annu. Rev. Earth Planet Sci.* **18**, 357 (1990).
- [4] Y. Fukai, *Nature (London)* **308**, 174 (1984).
- [5] T. Suzuki, S. Akimoto, and Y. Fukai, *Phys. Earth Planet. Inter.* **36**, 135 (1984).
- [6] Q. Williams and R. J. Hemley, *Annu. Rev. Earth Planet Sci.* **29**, 365 (2001).
- [7] O. Mathon, F. Baudalet, J. P. Itié, A. Polian, M. d'Astuto, J. C. Chervin, and S. Pascarelli, *Phys. Rev. Lett.* **93**, 255503 (2004).
- [8] K. Shimizu, T. Kimura, S. Furomoto, K. Takeda, K. Kontani, Y. Onuki, and K. Amaya, *Nature (London)* **412**, 316 (2001).
- [9] J. V. Badding, R. J. Hemley, and H. K. Mao, *Science* **253**, 421 (1991).
- [10] N. Ishimatsu, T. Shichijo, Y. Matsushima, H. Maruyama, Y. Matsuura, T. Tsumuraya, T. Shishidou, T. Oguchi, N. Kawamura, M. Mizumaki, T. Matsuoka, and K. Takemura, *Phys. Rev. B* **86**, 104430 (2012).
- [11] T. Matsuoka, N. Hirao, Y. Ohishi, K. Shimizu, A. Machida, and K. Aoki, *High Press. Res.* **31**, 64 (2011).
- [12] W. Mao, W. Sturhahn, D. Heinz, H. Mao, J. Shu, and R. Hemley, *Geophys. Res. Lett.* **31**, L15618 (2004).

- [13] C. Elsässer, J. Zhu, S. G. Louie, B. Meyer, M. Fähnle, and C. T. Chan, *J. Phys.: Condens. Matter* **10**, 5113 (1998).
- [14] N. Hirao, T. Kondo, E. Ohtani, K. Takemura, and T. Kikegawa, *Geophys. Res. Lett.* **31**, L06616 (2004).
- [15] A. G. Gavriluk, A. A. Mironovich, and V. V. Struzhkin, *Rev. Sci. Instrum.* **80**, 043906 (2009).
- [16] J. Y. Zhao, W. Bi, S. Sinogeikin, M. Y. Hu, E. E. Alp, X. C. Wang, C. Q. Jin, and J. F. Lin, *Rev. Sci. Instrum.* **88**, 125109 (2017).
- [17] W. Bi, J. Zhao, J. Lin, Q. Jia, M. Y. Hu, C. Jin, R. Ferry, W. Yang, V. Struzhkin, and E. E. Alp, *J. Synchrotron Radiat.* **22**, 760 (2015).
- [18] W. Sturhahn, *Hyperfine Interact.* **125**, 149 (2000).
- [19] G. Schneider, M. Baier, R. Wordel, F. E. Wagner, V. E. Antonov, E. G. Ponyatovsky, Yu. Kopilovskii, and E. Makarov, *J. Less-Common Met.* **172-174**, 333 (1991).
- [20] V. E. Antonov, M. Baier, B. Dorner, V. K. Fedotov, G. Grosse, A. I. Kolesnikov, E. G. Ponyatovsky, G. Schneider, and F. E. Wagner, *J. Phys.: Condens. Matter* **14**, 6427 (2002).
- [21] See Supplemental Material at <http://link.aps.org/supplemental/10.1103/PhysRevB.101.020405> for details of analyzing the XES spectra, which includes Refs. [22,23].
- [22] G. Vankó, T. Neisius, G. Molnár, F. Renz, S. Kárpáti, A. Shukla, and F. M. F. de Groot, *J. Phys. Chem. B* **110**, 11647 (2006).
- [23] J. Ying, H. Lei, C. Petrovic, Y. Xiao, and V. V. Struzhkin, *Phys. Rev. B* **95**, 241109(R) (2017).
- [24] J. P. Rueff, M. Krisch, Y. Q. Cai, A. Kaprolat, M. Hanfland, M. Lorenzen, C. Masciovecchio, R. Verbeni, and F. Sette, *Phys. Rev. B* **60**, 14510 (1999).